

# Implementation of a Standalone Solar Photovoltaic Hybrid System Using Fuzzy Logic Controller

G. Hanumantha Reddy<sup>1</sup>, P. Mounika<sup>2</sup>, P. Vinod Kumar<sup>3</sup>

<sup>1</sup>Assistant Professor, Department of EEE, SVEW, Tirupati.

<sup>2</sup>PG Scholar, Department of EEE, SVEW, Tirupati.

<sup>3</sup>Assistant Professor, Department of EEE, SVEW, Tirupati.

**ABSTRACT**--A control algorithm for a standalone solar photo-voltaic (PV)-diesel-battery hybrid system with Fuzzy Logic Controller is implemented in this paper. The proposed system deals with the intermittent nature of the energy generated by the PV array and it also provides power quality improvement. The PV array is integrated through a dc– dc boost converter and is controlled using a maximum power point tracking algorithm to obtain the maximum power under varying operating conditions. The battery energy storage system (BESS) is integrated into the diesel engine generator set for the coordinated load management and power flow within the system. The admittance-based control algorithm is used for load balancing, harmonics elimination, and reactive power compensation under three-phase four-wire linear and nonlinear loads. A four leg voltage-source converter with BESS also provides neutral current compensation. The performance of the proposed standalone hybrid system is studied under different loading conditions experimentally on a developed prototype of the system.

*Index Terms*—Admittance-based control algorithm, battery energy storage system (BESS), diesel generator (DG) set, four-leg voltage-source converter (VSC), neutral current compensation, power quality, solar photovoltaic (PV) array, standalone system.

## I. INTRODUCTION

A GLOBAL transition to renewable energy resources is well suited to meet the need for power in remote areas, which lack grid and road infrastructure. The support for the use of renewable energy resources is increasing as global warming is a major environmental concern, and it offers an alternative for future energy supply. Among the available renewable energy resources, solar photovoltaic (PV) power generation is gaining wide acceptance, and it is used for various applications such as household appliances, remote missions, data communications, telecommunication systems,

hospitals, electric aircraft, and so-lar cars [1]. The utilization of the PV power generation is for the reason that it has many advantages such as it gives clean power, is portable in nature, and can be employed for various small-scale applications [2]. However, considering the large fluctuations in the output of PV power, it is imperative to integrate other power sources like a diesel generator (DG) set, battery storage, fuel cells, etc. The performance analysis of standalone systems with PV- and DG-based sources is given in [3]. The design and operation of standalone DG-SPV-battery energy storage (BES) using a peak detection based control approach is shown in [4]. A character triangle function (CTF)-based control approach and its analysis for four-wire standalone distribution system are demonstrated in [5].

An enhanced phase-locked loop (EPLL)-based control approach is shown in [6], wherein three EPLLs are used for extraction of fundamental active and reactive power components of load currents. However, only simulation studies are presented in [4]–[6]. A composite observer-based control approach for standalone PV-DG-based system is used in [7]. However, the authors have provided experimental results, but the control approach in [7] is complex and requires tuning of internal parameters. Unlike the control approach in [7], the proposed system uses a conductance-based simple control approach. Moreover, a detailed experimental study is used to demonstrate all the features of the system. The proposed system consists of a diesel-engine-driven permanent magnet synchronous generator (PMSG), PV array, and BES. This microgrid is a representative of a typical rural hospital power supply system which needs to ensure uninterrupted constant power supply for  $24 \times 7$  h. Therefore, the PMSG driven by a diesel engine ensures regulated power supply. In order to maintain the efficiency and to reduce the maintenance cost, the DG set is made to operate at 80–100% of its full capacity [8]. This is because, under light-load conditions, the efficiency reduces and the maintenance cost also increases as the DG set is subjected to carbon build up. Usually, to avoid these problems, the DG is operated by keeping a minimum loading of 80% by means of battery

charging or the DG is made to turn ON/OFF depending upon the loading [9]–[11]. However, the turn ON/OFF of the DG set is usually not recommended as [12], [13].

1) The load may vary frequently. Therefore, the repeated turn ON/OFF of DG increases the mechanical maintenance.

2) The battery life reduces as the discharging current is high during transient periods.

Besides, the PMSG driven by the diesel engine does not require a separate excitation control. The machine is robust, efficient, brushless construction, and with less maintenance [14]. A battery energy storage system (BESS) is incorporated to provide load leveling in the case of variations in PV array output power.

The BESS is considered as ideal energy storage for a standalone system as compared to compressed air, super capacitors, fly-wheels, pumped hydro, and superconducting magnetic storage [15]–[17]. The implementation of a standalone system devised of PV array, DG set, and BESS intends to fulfill the following requirements

1) To control the point of common coupling (PCC) voltage depending upon the solar irradiance variations, and load fluctuations and unbalances.

2) There is no requirement for the measurement of load for turn ON/OFF of DG.

3) The power quality of the system is improved by reducing the total harmonic distortion (THD) of PCC voltages and DG set currents under IEEE-519 standard.

4) To effectively regulate power flow between source and load.

5) The voltage-source converter (VSC) of BESS provides reactive power compensation and maintains the balanced DG currents. This reduces the vibration of shaft and over-heating of machines.

6) It allows neutral current compensation using four leg VSC.

Nowadays, the rapid increase in the use of nonlinear loads such as computers, electronics appliances, medical equipment, refrigerators, etc., has emphasized the concern for power quality in the electrical distribution system. These loads inject harmonics and distort the current and voltage waveforms causing poor power quality problems. The possible provision for the mitigation of the power quality problems is with inclusion of custom power devices [18] while meeting the IEEE-519 standard. Three-phase four-wire loads are also known to suffer from the problem of neutral current due to nonlinearity and unbalance present in the system. This may produce large amount of neutral current which consists of triplen harmonics. The neutral current may cause overloading of the distribution system and causes additional heat losses, which may be dangerous and poses a serious threat to the connected equipment. A four-leg VSC is used for neutral

current compensation in addition to mitigate the current harmonics with other reported advantages [19].

Additionally, the flexible operation of the system depends upon implementation of the various control strategies. Some of the control algorithms that have been applied for controlling are multi loop strategy [20], sliding-mode control [21], P controller-based technique [22], FLC-based control method [23], and enhanced phase locked technique [24]. The authors have failed to discuss the power quality and reactive power compensation. The response of these controllers to the unbalance and dynamic conditions is slow.

In this paper, an admittance-based control algorithm [25] is applied for the evaluation of reference power component of source currents in the PV-DG hybrid system. The admittance of the load is estimated using the active and reactive powers of the load. The conductance (GL) and susceptance (BL) are extracted from the estimated active power and reactive power of the three-phase four-wire loads, respectively. It is a simple mathematical formulation based on sinusoidal Fryze current control. This control strategy is based on the Lagrange's multiplier method and the fundamental principle of the PQ theory where the computation through the Clarke's transformation is eliminated. Therefore, it provides an improvement in the mathematical calculations. Here, the inputs are the load currents ( $i_{L a}$ ,  $i_{L b}$ ,  $i_{L c}$ ) and load voltages ( $v_a$ ,  $v_b$ ,  $v_c$ ), which are further used for the estimation of the active (p) and reactive (q) power components using the formula mentioned in this paper. The oscillating component of power is eliminated as it is passed through the low-pass filter (LPF) to obtain  $P_{dc}$  and  $Q_{dc}$ . These are used for the estimation of the reference conductance and susceptance, thus giving the value for the reference active and reactive power components. This method facilitates the extraction of the fundamental components and compensates independently for the active and reactive powers even when the system comprises of harmonics and unbalances at the PCC. The compensation allows balanced source currents to be drawn from the network. The controller responds faster under the steady-state and dynamic conditions. The control implementation is realized using a four-leg VSC with admittance control algorithm. The performance is verified experimental study using digital signal processor (DSP-dSPACE) under both linear and nonlinear loads.

## II. SYSTEM DESIGN AND CONFIGURATION

The standalone system consists of a PV array along with a boost converter, maximum power point tracking (MPPT) controller, diesel-engine-driven PMSG, a four-leg VSC with BESS, and three-phase four-wire ac loads as shown in Fig. 1. The voltage at the PCC is restored by coordinating the reactive power through VSC control. Under varying conditions of generation and loads, BESS offers charging during the daytime when the insolation is large and the load is less. The battery discharges to compensate for any deficits. The DG set operates while maintaining the system frequency

under varying generation and loads. The terminal capacitor provides a constant rated terminal voltage at no load. A four-leg VSC is interfaced along with its dc bus. The ripple filter and interfacing inductors are used to eliminate the switching harmonics.

MPP. The MPPT controller regulates the control signal of the dc–dc boost converter until the following condition is satisfied:

$$(\partial I/\partial V) = -(I/V). \tag{1}$$

**B. Boost Converter**

The design parameters for a boost converter depend upon the current ripple, voltage ripple, and power rating. The boost converter is interfaced with MPPT controller for tracking the maximum power.

It is used to boost the voltage to 400 V to feed power to the battery.

The inductor of the boost converter is given as

$$L_b = \frac{V_{in}DT}{\Delta I} = \frac{165 \times 0.5875 \times 1 \times 10^{-4}}{0.1 \times 27.27} = 3.55 \text{ mH} \approx 4 \text{ mH} \tag{2}$$

Where  $V_{in}$  is the input voltage.  $D$  is the duty cycle,  $T$  is the time period, and  $\Delta I$  is the inductor ripple current. The value of  $\Delta I$  is taken as 10% of the input current. The variation caused by the ripples on the PV power is taken care with the addition of a capacitor ( $C$ ) at the input of the boost converter as shown in Fig. 1. This absorbs the ripples and smoothen the power flow within the system.

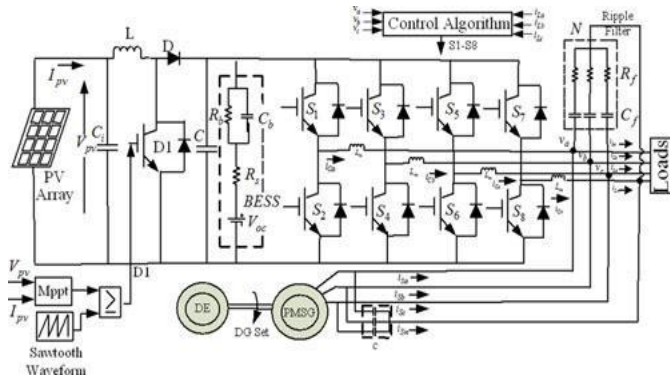


Fig. 1. Schematic diagram of the proposed system.

The considerations required for the selection of various elements are discussed as follows and their values are given in the Appendix.

**A. Solar PV Array**

The PV array is essentially modeled with the series and parallel modules where insolation and ambient temperature acts as

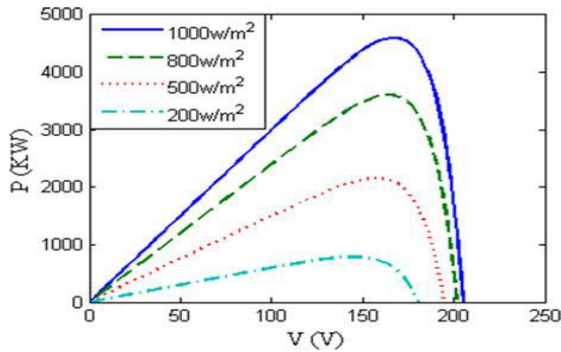


Fig. 2. PV characteristics.

Input [26]. The light-generated current of the PV array depends linearly on the solar irradiation and is also influenced by the temperature as shown in Fig. 2. There are ten modules in series resulting in 205 V under open-circuit condition and 100 modules are connected in parallel for 30-A short circuit current in the PV array. The PV array has been provided with a MPPT controller in order to operate at the maximum power point (MPP) at any given temperature and insolation level. The incremental conductance (IC) algorithm tracks the voltage and current at the maximum power of the solar [27]. This IC method performs good with noise rejection and less confusion due to system dynamics. The IC method has been used here, which presents the MPP depending upon the slope of the power curve. The slope of the curve is zero at

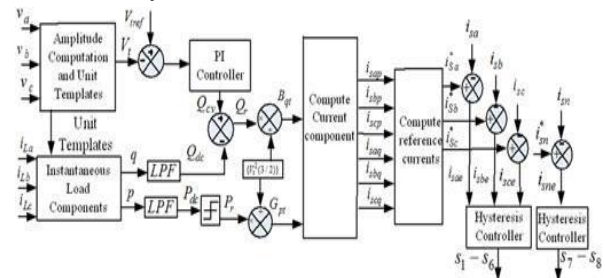


Fig. 3. Admittance-based control algorithm.

**C. Battery Energy Storage System**

The battery is connected at the dc link of the VSC. The battery is an energy storage unit, its energy is represented in kilowatt-hour, and a capacitor is used to model the battery unit as shown in Fig. 1. A 2.8-kWh capacity battery rack is used for the energy storage. Therefore, 36 sections of 12 V and 7 Ah are connected in series. The parallel configuration of  $R_b$  and  $C_b$  describes the charging/discharging stored energy and voltage. The value of resistance  $R_b = 10 \text{ k}\Omega$  is large, while  $R_s = 0.1 \text{ W}$  is very small for all practical purposes. The battery operates according to the load variations. In conditions, when the load demand has increased, under those conditions, the power stored in the battery is used, and therefore, the battery starts discharging according to its discharge rate. In the case of reduced load demand, the battery charges from the available PV power once the load demand is satisfied.

### D. Ripple Filter

The first-order LPF is tuned at half the switching frequency. It is used to filter the switching ripples of a VSC at PCC. The selected switching frequency is 10 kHz. The switching frequency of 10 kHz is selected, as it would give reduced losses and the size of the components is appropriate according to the selected switching frequency as compared to other value of switching frequency. The value of capacitor is taken as 10 μF. The ripple filter consists of a resistor in series with the capacitor. The value of the resistor is considered to be 5 Ω.

### III. CONTROL ALGORITHM

The control algorithm extracts the fundamental component of the loads using the admittance control technique. Further, active and reactive power components of the load currents are determined. The proportional integral (PI) control loop produces reactive power ( $Q_{cv}$ ) for voltage control in order to compensate for any changes in reactive power in support to fluctuations in PCC voltages. The reference susceptance ( $B_{qt}$ ) for reactive component of source current is computed by deducting the three phase load reactive power ( $Q_{dc}$ ) from the PI controller output ( $Q_{cv}$ ). The reference conductance ( $G_{pt}$ ) is estimated using the reference load active power ( $P_r$ ). The load active power component is limited to operate the DG set at 80–100% of its full-load capacity with VSC-BESS allowing load leveling. Fig. 3 shows the block diagram of the control technique.

The evaluation of the control algorithm demonstrates its robustness and relatively faster response. As it is the simple estimation of the active and reactive power components, the quality of computation is increased. Further, while working with the mathematical calculations, there is no delay for obtaining the results and the occurrence of error within the system is also reduced. Therefore, the system performance improves with this control algorithm.

#### A. Determination of Unit Templates

The amplitude of PCC voltage  $V_t$  and phase voltages are employed for the computation of in-phase unit template

$$V_t = \sqrt{\{2 \times (v_a^2 + v_b^2 + v_c^2)/3\}} \quad (3)$$

$$u_a = \frac{v_a}{V_t}, \quad u_b = \frac{v_b}{V_t}, \quad u_c = \frac{v_c}{V_t}. \quad (4)$$

The quadrature unit templates are estimated as

$$w_a = (-u_a + u_c)/\sqrt{3} \quad (5)$$

$$w_b = (3u_a + u_b - u_c)/2\sqrt{3} \quad (6)$$

$$w_c = (-3u_a + u_b - u_c)/2\sqrt{3}. \quad (7)$$

#### B. Admittance Control Technique

The instantaneous load active power (p) and load reactive power (q) components are computed as follows. The calculated instantaneous components of load power consist of

ac and dc components. The dc components are extracted using LPF

$$p = \{v_t(u_a i_{La} + u_b i_{Lb} + u_c i_{Lc})\} = P_{dc} + P_{ac} \quad (8)$$

$$q = -\{v_t(w_a i_{La} + w_b i_{Lb} + w_c i_{Lc})\} = Q_{dc} + Q_{ac}. \quad (9)$$

The voltage error for the k<sup>th</sup> instant at PCC is given as

$$V_e(k) = V_{tref}(k) - V_t(k) \quad (10)$$

Where  $V_{tref}(k)$  is the terminal ac reference voltage amplitude and  $V_t(k)$  is the amplitude of three-phase sensed ac voltages at PCC as given in (10).

The PI controller output for maintaining the PCC voltage at the k<sup>th</sup> sampling instant is given as

$$Q_{cv}(k) = Q_{cv}(k-1) + k_{pv} [V_e(k) - V_e(k-1)] + k_{iv} V_e(k) \quad (11)$$

Where  $k_{pv}$  and  $k_{iv}$  denote the proportional and integral gains of the PI controller.

The reference reactive power component ( $Q_r$ ) is computed from the difference of the PI controller output ( $Q_{cv}$ ) and the load reactive power component ( $Q_{dc}$ ) as

$$Q_r = Q_{cv} - Q_{dc}. \quad (12)$$

The active power drawn from the DG set ( $P_r$ ) is limited to  $0.8P_R \leq P_{dc} \leq 1.0P_R$ . The reference source active power The reference conductance ( $G_{pt}$ ) and susceptance ( $B_{qt}$ ) of the load corresponding to the reference active ( $P_r$ ) and reactive power ( $Q_r$ ) components are derived as

$$G_{pt} = P_r / \{V_t^2(3/2)\} \quad (13)$$

$$B_{qt} = Q_r / \{V_t^2(3/2)\} \quad (14)$$

$$i_{sap} = G_{pt} V_t u_a, \quad i_{sbp} = G_{pt} V_t u_b, \quad i_{scp} = G_{pt} V_t u_c \quad (15)$$

$$i_{saq} = B_{qt} V_t w_a, \quad i_{sbq} = B_{qt} V_t w_b, \quad i_{scq} = B_{qt} V_t w_c. \quad (16)$$

The total reference source currents ( $i^*S_a, i^*S_b, i^*S_c$ ) are obtained as sum of in-phase and quadrature components of reference source currents of individual phases as

$$i^*S_a = i_{sap} + i_{saq}, \quad i^*S_b = i_{sbp} + i_{sbq}, \quad i^*S_c = i_{scp} + i_{scq}. \quad (17)$$

### C. Neutral Current Compensation

This fourth leg of VSC provides direct control over the source neutral current. The reference neutral current ( $i^*S_n$ ) is compared with the sensed source neutral current ( $i_{sn}$ ), as shown in Fig. 3. These are used in hysteresis current controller to produce switching signals for four leg of VSC.

### IV. FUZZY LOGIC CONTROLLER



Fuzzy logic uses fuzzy set theory, in which a variable is member of one or more sets, with a specified degree of membership. Fuzzy logic allow us to emulate the human reasoning process in computers, quantify imprecise information, make decision based on vague and in complete data, yet by applying a “defuzzification” process, arrive at definite conclusions.

The FLC mainly consists of three blocks

- Fuzzification
- Inference
- Defuzzification
- 

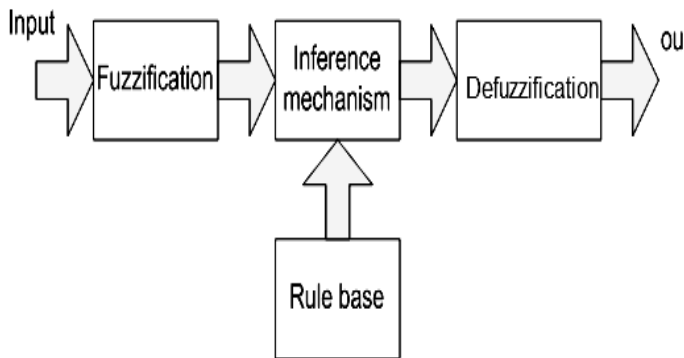


**Fig. 4 Block Diagram of a Fuzzy Logic Controller**

**RULES:**

If input is NEGATIVE then output is POSITIVE

If input is ZERO then output is ZERO

If input is POSITIVE then output is NEGATIVE

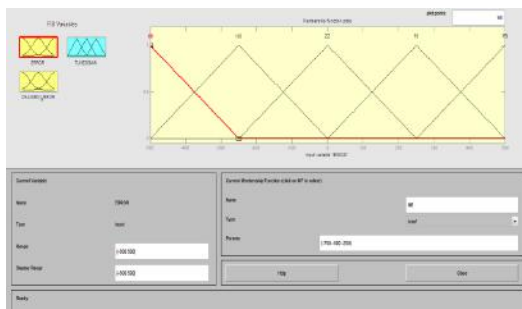


**Fig..5 Fuzzy Inputs and Outputs**

**V. SIMULATION RESULTS**

The response of a standalone system is analyzed under nonlinear load using simpowersystem toolbox in MATLAB/SIMULINK. The performance of the system is observed during line outage in one of the three phases at time  $t = 1.5$  s to 1.56 s, as shown in Fig. 7.

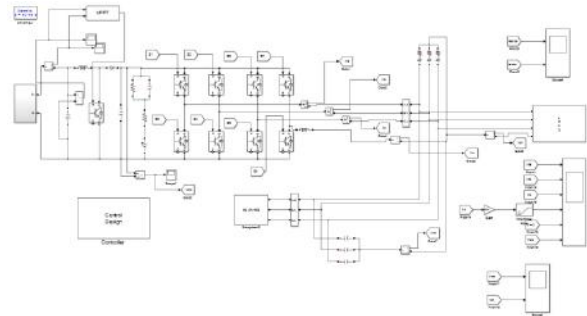


**Fig 6.MATLAB/SIMULINK Model for the proposed System**

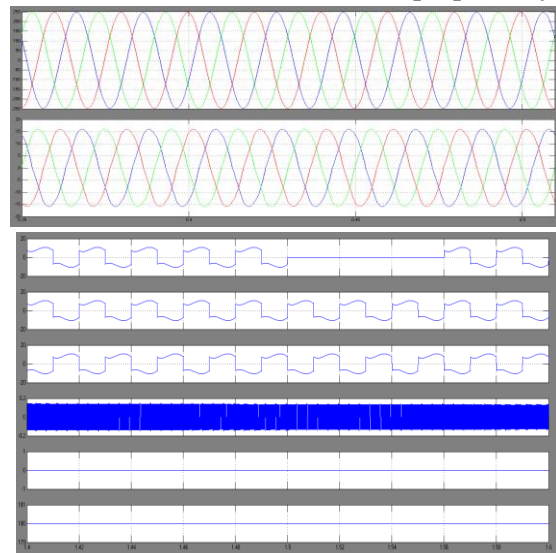


**Fig. 7. Performance of the proposed system under unbalance nonlinear load.**

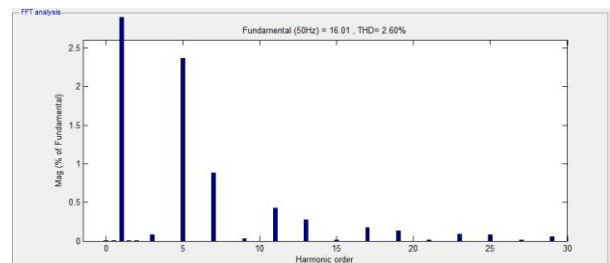


**Fig8. THD values of Source Current**

It is observed that for a subjected load unbalance in the system, the four-leg VSC has the capability of harmonics elimination as the source currents and the source voltages are maintained constant and neutral current compensation is provided while maintaining a zero source neutral current. The neutral current compensation provided by the four-leg VSC is

clearly illustrated with the variations in the load neutral current and VSC neutral current waveforms. The system maintains its PCC voltage at the desired level. Moreover, it should be noted that even during unbalanced loading, the supply currents are balanced and sinusoidal there by leading to balanced loading on the DG, which in turn results in reduced maintenance and improved efficiency of DG.

## VI. CONCLUSION

The admittance-based control technique has been used for a PV-diesel-battery hybrid system with Fuzzy Logic Controller (FLC) for an uninterrupted power supply and power quality improvement. The incremental based MPPT algorithm has delivered maximum solar array power under varying conditions of temperature and insolation radiation. The technique has been demonstrated to eliminate harmonics, load balancing, and to provide neutral current compensation by incorporating four-leg VSC in the system. The PCC voltage and frequency have been maintained constant. Satisfactory performance of the system has been observed through test results obtained for steady-state and dynamic conditions under both linear/nonlinear loads.

## REFERENCES

- [1] Z. Jiang, "Power management of hybrid photovoltaic-fuel cell power systems," presented at the IEEE Power Eng. Soc. Gen. Meeting, Montreal, QC, Canada, 2006.
- [2] A. Naik, R. Y. Udaykumar, and V. Kole, "Power management of a hybrid PEMFC-PV and ultra capacitor for stand-alone and grid connected applications," in *Proc. IEEE Int. Conf. Power Electron. Drives Energy Syst.*, 2012, pp. 1–5.
- [3] J. Philip *et al.*, "Control and implementation of a standalone solar photovoltaic hybrid system," in *Proc. IEEE Ind. Appl. Soc. Annu. Meeting*, Addison, TX, USA, Oct. 18–22, 2015, pp. 1–8.
- [4] J. Philip, B. Singh, and S. Mishra, "Design and operation for a standalone DG-SPV-BES microgrid system," in *Proc. 6th IEEE Power India Int. Conf.*, New Delhi, India, Dec. 5–7, 2014, pp. 1–6.
- [5] J. Philip, B. Singh, and S. Mishra, "Analysis and control of an isolated SPV-DG-BESS hybrid system," in *Proc. 6th IEEE India Int. Conf. Power Electron.*, Kurukshetra, India, Dec. 8–10, 2014, pp. 1–6.
- [6] J. Philip, B. Singh, and S. Mishra, "Performance evaluation of an isolated system using PMSG based DG set, SPV array and BESS," in *Proc. IEEE Power Electron., Drives Energy Syst.*, Mumbai, India, Dec. 16–19, 2014, pp. 1–6.
- [7] J. Philip, K. Kant, C. Jain, B. Singh, and S. Mishra, "A simplified configuration and implementation of a standalone microgrid," in *Proc. IEEE Power Energy Soc. Gen. Meeting*, Denver, CO, USA, Jul. 26–30, 2015, pp. 1–5.
- [8] B. Singh and R. Niwas, "Power quality improvements in diesel engine driven induction generator system using SRF theory," in *Proc. 5th IEEE Power India Conf.*, 2012, pp. 1–5.
- [9] R. Pena, R. Cardenas, J. Probst, J. Clare, and G. Asher, "Wind-Diesel generation using doubly fed induction machines," *IEEE Trans. Energy Convers.*, vol. 23, no. 1, pp. 202–214, Mar. 2008.
- [10] R. Tonkoski, L. A. C. Lopes, and D. Turcotte, "Active power curtailment of PV inverters in diesel hybrid mini-grids," in *Proc. IEEE Elect. PowerEnergy Conf.*, Oct. 22–23, 2009, pp. 1–6.
- [11] N. A. Ninad and L. A. C. Lopes, "A BESS control system for reducing fuel consumption and maintenance costs of diesel hybrid mini-grids with high penetration of renewables," in *Proc. IEEE ECCE Asia Downunder*, Melbourne, Australia, 2013, pp. 409–415.
- [12] M. Datta, T. Senju, A. Yona, T. Funabashi, and C.-H. Kim, "A coordinated control method for leveling PV output power fluctuations of PV-diesel hybrid systems connected to isolated power utility," *IEEE Trans. Energy Convers.*, vol. 24, no. 1, pp. 153–162, Mar. 2009.
- [13] S. G. Malla and C. N. Bhende, "Enhanced operation of stand-alone photovoltaic-diesel generator-battery system," *J. Elect. Power Syst. Res.*, vol. 107, pp. 250–257, Feb. 2014.
- [14] B. Singh and S. Sharma, "An autonomous wind energy conversion system with permanent magnet synchronous generator," in *Proc. IEEE Int. Conf. Energy, Autom. Signal*, Bhubaneswar, India, 2011, pp. 1–6.
- [15] M. Datta, T. Senju, A. Yona, and T. Funabashi, "Photovoltaic output power fluctuations smoothing by selecting optimal capacity of battery for a diesel hybrid system," *Elect. Power Compon. Syst.*, vol. 39, pp. 621–644, 2011.
- [16] S. C. Smith, P. K. Sen, and B. Kroposki, "Advancement of energy storage devices and applications in electrical power system," in *Proc. IEEE PowerEnergy Soc. Gen. Meeting, Convers. Del. Elect. Energy 21st Century*, 2008, pp. 1–8.
- [17] G. Wang, M. Ciobotaru, and V. G. Agelidis, "PV power plant using hybrid energy storage system with improved efficiency," in *Proc. 3rd IEEE Int. Symp. Power Electron. Distrib. Gener. Syst.*, 2012, pp. 808–813.
- [18] K. R. Padiyar, *FACTS Controllers in Power Transmission and Distribution*. New Delhi, India: New Age Int., 2008.
- [19] R. R. Sawant and M. C. Chandorkar, "A multifunctional four-leg grid connected compensator," *IEEE Trans. Ind. Appl.*, vol. 45, no. 1, pp. 249–259, Jan./Feb. 2009.
- [20] H. Mahmood, D. Michaelson, and J. Jiang, "Control strategy for a standalone PV/battery hybrid system," in *Proc. 38th IEEE Annu. Conf. Ind. Electron. Soc.*, 2012, pp. 3412–3418.
- [21] Y. Mi, Y. Fu, J. B. Zhao, and P. Wang, "The novel frequency control method for PV-diesel hybrid system," in *Proc. 10th IEEE Int. Conf. Control Autom.*, Jun. 2013, pp. 180–183.
- [22] M. Zahran, O. Mahgoub, and A. Hanafy, "P-controller based photovoltaic battery diesel (PVBD) hybrid system management and control," in *Proc. 35th Intersoc. Energy Convers. Eng. Conf. Exhib.*, 2000, vol. 2, pp. 1513–1521.
- [23] M. Zahran, A. Hanafy, O. Mahgoub, and M. Kamel, "FLC based photovoltaic battery diesel hybrid system management and control," in *Proc. 35th Intersoc. Energy Convers. Eng. Conf. Exhib.*, 2000, vol. 2, pp. 1502–1512.
- [24] S. Sharma and B. Singh, "An enhanced phase locked loop technique for voltage and frequency control of stand-alone wind energy conversion system," in *Proc. Int. Conf. Power Electron.*, 2011, pp. 1–6. PHILIP *et al.*: CONTROL AND IMPLEMENTATION OF A STANDALONE SOLAR PHOTOVOLTAIC HYBRID SYSTEM 3479
- [25] B. Singh and S. Arya, "Admittance based control algorithm for DSTATCOM in three phase four wire system," in *Proc. 2nd Int. Conf. Power, Control Embedded Syst.*, 2012, pp. 1–8.

[26] M. Suthar, G. K. Singh, and R. P. Saini, "Comparison of mathematical models of photovoltaic (PV) module and effect of various parameters on its performance," in *Proc. IEEE Int. Conf. Energy Efficient Technol. Sustain.*, 2013, pp. 1354–1359.

**Mr.G.Hanumantha Reddy** is currently working as an Assistant Professor in EEE department, SV ENGINEERING COLLEGE FOR WOMEN, Tirupati. He has received his bachelor of Technology (B.tech) from Sreenivasa Institute of Technology And Management Science, Chittoor, AP, India in 2007 and M.Tech degree in Electrical Power Systems, MITS, Madanapalle, AP, India in 2012. His areas of interest include Power Systems.

**P.Mounika** is currently pursuing her Master of Technology in Power Systems, EEE Department, S V Engineering College For Women, Karakambadi Road, Tirupati, Andhra Pradesh, India. She has received his bachelor of Technology (B.tech) from, S V Engineering College For Women, Karakambadi Road, Tirupati, Andhra Pradesh, India in 2015.

**Mr.P.Vinod Kumar** is currently working as an Assistant Professor in EEE department, SV ENGINEERING COLLEGE FOR WOMEN, Tirupati. He has received his bachelor of Technology (B.tech) from KSRM College of Engineering, Kadapa, AP, India in 2003 and M.Tech degree in Power Systems, N.I.T. Jamshedpur, Jamshedpur, India in 2008. His areas of interest include Power Systems.